LUNAR ALBEDO RECONSTRUCTION FROM APOLLO METRIC CAMERA IMAGES

Ara V. Nefian, Oleg Alexandrov, Ross Beyer, Zachary Moratto, Trey Smith, Michael Broxton, Randolph Kirk and Mark Robinson

The goal of this proposal is to fully realize the potential of the Apollo Metric Camera system by developing a high resolution (10m/pixel), large coverage (16% of the Lunar surface) albedo map of the Lunar surface. Our proposal is made possible by the digital scans of Apollo imagery made recently available at NASA JSC and Arizona State University and by the automatic processing of high accuracy digital terrain models (DTM) of the Lunar surface from these scanned Apollo imagery [1] developed at NASA ARC. Drawing on these extraordinary resources and the advances in Lunar reflectance modeling, we use the latest digital image processing and photometric techniques, with a high degree of automation, to

- Generate a validated *Digital Albedo Model* from the Apollo Metric Camera imagery covering at least 16% of the Moon, at an unprecedented resolution of 10–20 m/pixel, that (a) compensates for the effect of variable exposure time, illumination conditions, and shadows; (b) has albedo geodetically aligned to the Clementine global base map, so that the new data set can be used as a high-resolution overlay consistent with the existing global data set; and (c) has a confidence map associated with the reconstructed albedo map.
- Generate an *Enhanced Digital Terrain Model* for the same area at a resolution of 30–40 m/pixel, built by applying statistical denoising techniques to overlapping areas in existing local DTMs, along with a confidence map estimating the DTM error. This enhanced DTM eliminates artifacts and improves resolved terrain detail in the the existing LMMP-funded DTM.
- Document these data products and submit them in a suitable format to PDS.

All goals of this grant (NASA Proposal Number 09-LASER09-0092) have been accomplished as described in the following sections of this report. Section 1 describes in more detail each of the above products and their specifications. Section 2 presents the technical papers published in various image processing and planetary science conferences as a result of this research work. Section 3 illustrates the technical approach used to accomplish these products. Section 4 refers the users to a new publicly available software library that has been build to generate the products funded by this grant. This software library generalizes to several planetary data sources and can be used to generate similar products from current and future NASA and international missions.

1 Accomplished and Delivered Products

1.1 Validated Digital Albedo Model from the Apollo Metric Camera Imagery

The main results of this grant are the release of the Lunar albedo (Figure 1) reconstructed from images taken by the Apollo Metric Camera flown onboard the Apollo 15, 16 and 17 missions, together with the confidence map (Figure 2). This derived data product covers an approximate 16% of the Lunar surface at an unprecedented resolution of 10mpp for this coverage. For comparison, LRO-WAC albedo mosaic covers 100% of the Lunar surface at 100mpp and the current LRO-NAC derived albedo mosaic covers about 2% of the Lunar surface at 1mpp resolution. Compared to imagery obtained from more recent missions, the images captured on film by Apollo missions have more noise artifacts and errors in camera position and orientation and exposure time making the processing of this data significantly more challenging. To deal with these noise sources, the team of this proposal developed and improved on a set of data processing tools (Vision Workbench Ames Stereo Pipeline and Photometry Toolkit) that are also released in open source. The overall albedo reconstruction is shown in Figure 1 over the Clementine mission mosaic. It is important to note the seamless derived albedo mosaic as well as the almost seamless transition between Apollo reconstructed albedo and Clementine image mosaic. Figures 3 and 4 present in more detail differences between the image mosaic (left) and the reconstructed albedo mosaic [2] using the techniques described in Section 3. Together with the albedo mosaic we released the confidence map consisting of alebdo reconstructed error (Figure 2) described in Section 3, Equation 9 and associated with each pixel of the albedo mosaic.

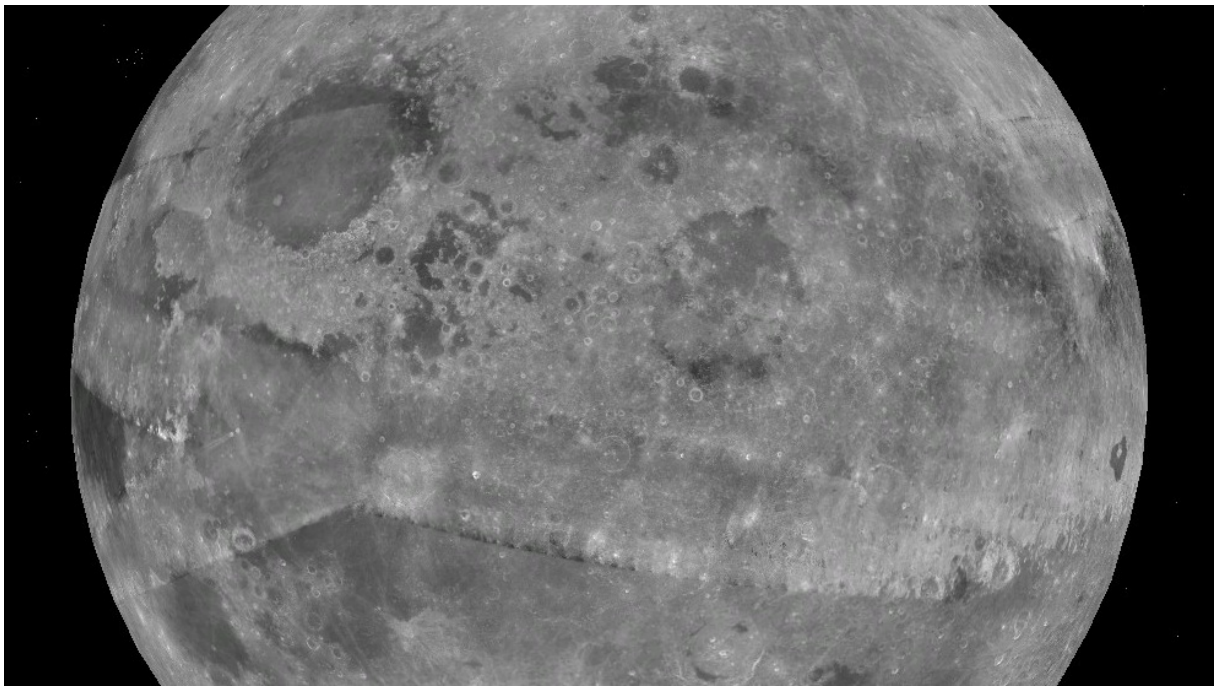

Figure 1: Final albedo reconstruction results of the Apollo zone.

The Lunar albedo and the corresponding confidence map files can be accessed in geotif tile format from

https://byss.arc.nasa.gov/albedo/albedo_10mpp_06_20_2012/albedo

and

https://byss.arc.nasa.gov/albedo/albedo_10mpp_06_20_2012/error

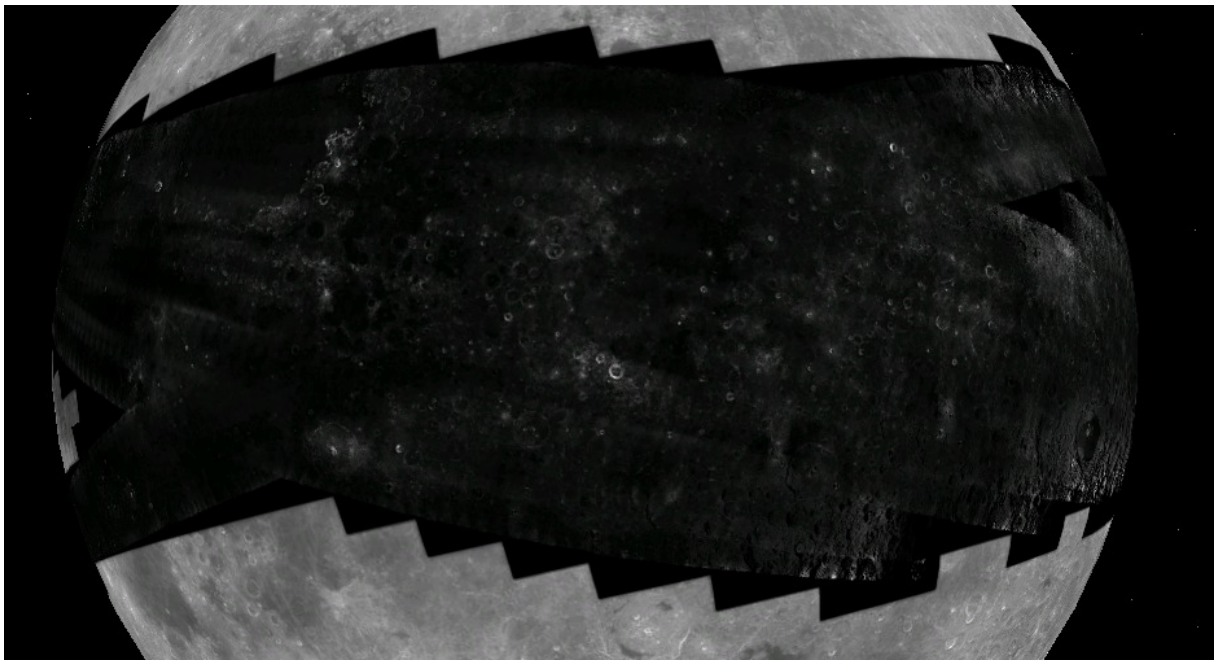

Figure 2: Confidence map for the reconstructed albedo.

respectively. The albedo in KML format (viewable in Google Earth) can be accessed at

https://byss.arc.nasa.gov/albedo/kml/albedo_10mpp_06_20_2012/albedo_10mpp_06_20_2012.kml

1.2 Enhanced Digital Terrain Model from the Apollo Metric Camera Imagery

The albedo mosaic relies on accurate terrain model for the computation of local normals. The terrain model is obtained using stereo pairs formed by consecutive images in each Apollo mission orbit. The resulting terrain models are further overlapping with terrain models derived from stereo pairs within the same orbit, adjacent orbits or other missions. The enhanced DTM of the Apollo Metric Camera Imagery combines all above terrain models using a statistical technique detailed in Section 3.2. Figure 1.2 illustrates the color-shaded relief of the enhanced DTM corresponding to the Apollo 15, 16 and 17 missions. The DEM tiles are available at https://byss.arc.nasa.gov/albedo/DEM.

1.3 Documentation of the Data Products and Public Release

The products generated by this grant (albedo mosaic, albedo mosaic precision and enhanced terrain model) have been documented and uploaded in to the Lunar Mapping and Modeling Portal at www.lmmp.nasa.gov and made publicly available. The team of this proposal is currently in the final stages of formatting and releasing these products to the Planetary Data System.

2 Publications

The scientific results and technical approach used in this research work were published in several planetary science and computer vision conferences: [3], [4], [2], [5], and [6].

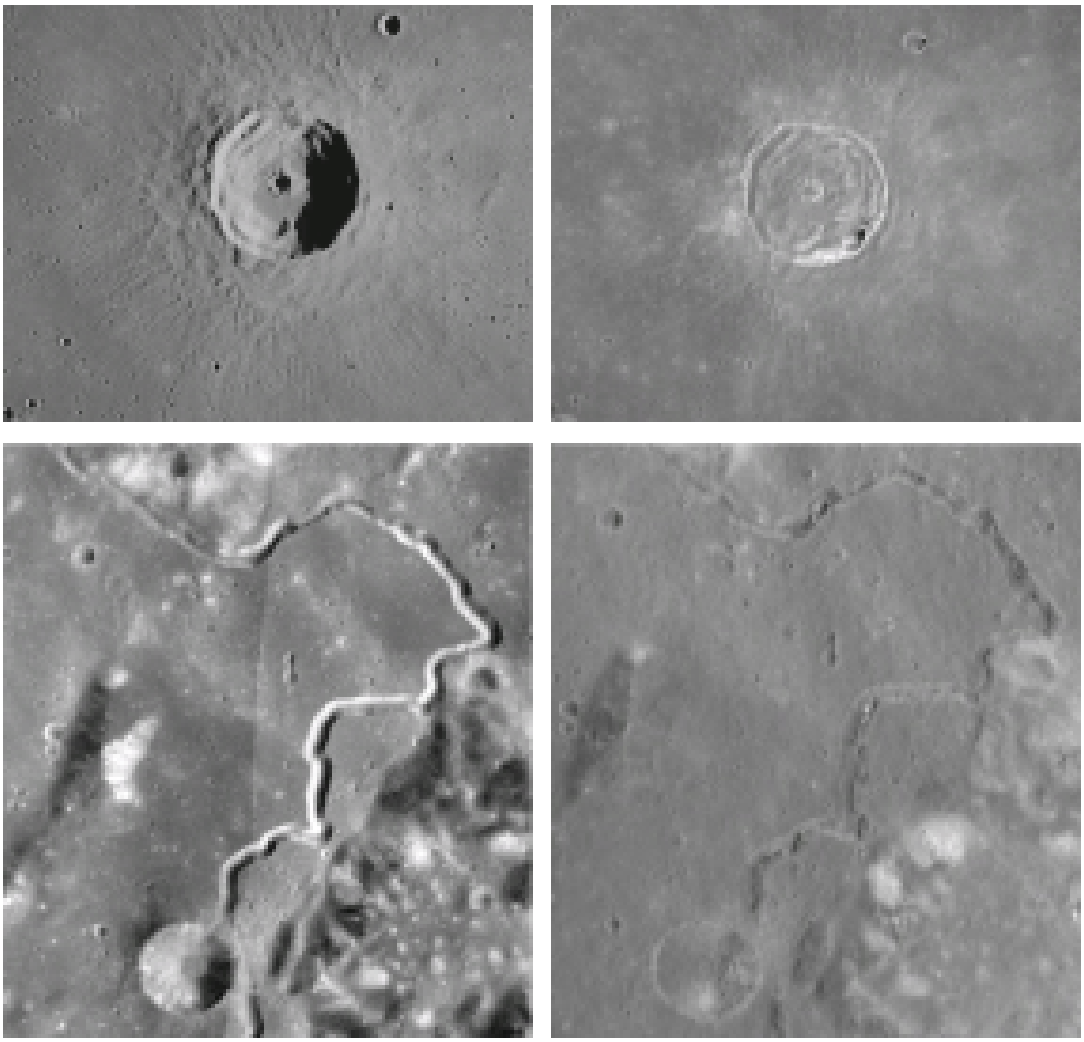

Figure 3: Image mosaic of the Apollo zone (left), and the reconstructed albedo (right).

3 Technical Approach

Each pixel of the Apollo Metric Camera images was formed by a combination of many factors, including albedo, terrain slope, exposure time, shadowing, and viewing and illumination angles. The goal of albedo reconstruction is to separate the contributions of these factors. This is possible in part because of redundancy in the data; specifically, the same surface location is often observed in multiple overlapping images. The albedo reconstruction technique includes all of the above factors in a image formation model and re-estimates them from the existing imagery. The overall system illustrated in this report is shown in Figure 3. The components of this block diagram are explained in more detail in the following sections.

3.1 Shadow Map Computation

Discarding unreliable image pixels that are in shadow and for which the DEM and the reflectance models are unreliable plays an important role in accurate albedo estimation [7, 8]. Figure 9 (left, middle) shows an input image together with its binary shadow map; shadowed areas are indicated in white. Figure 3 top shows an example of shadow removal and mosaicing from adjacent images that is able to retrieve visual

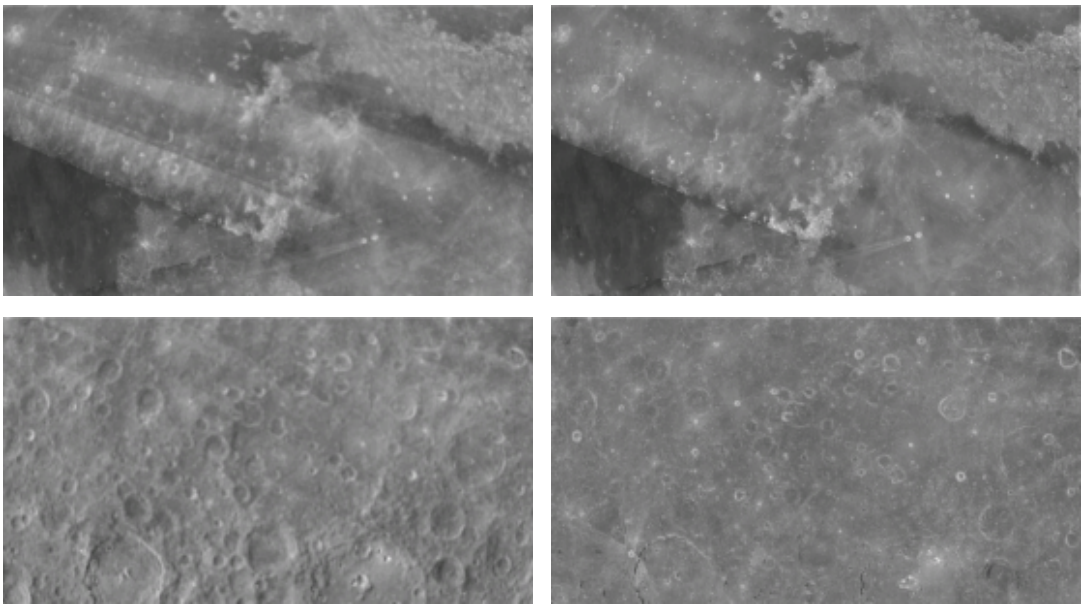

Figure 4: Image mosaic of the Apollo zone (left), and the reconstructed albedo (right).

information in areas originally occluded by shadows.

3.2 Enhanced Digital Terrain Model Computation

The geodetically aligned local DTM (extracted from a single stereo pair) determine multiple values for the same location on the Lunar surface. A weighted average of the local DTM value determines the value used in computing the local slopes and the reflectance value. The weights are float positive numbers smaller than unit associated with each post in a local DTM. They decrease linearly from the center to the edges. The weighted average DTM has the following benefits for albedo reconstruction:

- It is essential to the computation of a coherent photometric function since each point of the Lunar surface must have a unique elevation value.
- The statistical process produces more accurate terrain models by reducing the effect of random errors in local DEMs and without blurring the topographical features. Figure 7 shows the shaded subregion of the orbital image in Figure 9 before and after the weighted DTM averaging and denoising process. It can be seen that the noise artifacts in the original DTM are reduced in the denoised DEM while the edges of the large crater and mountain regions are very well preserved.
- The statistical parameters of the DTM values at each point are instrumental in building a confidence map of the Apollo coverage DTM. Figure 9 (right) shows the error confidence map for the orbital image illustrated in Figure 9 (left). The values shown in this error map are $0.05\times$the variance values of the DEM expressed in meters.

3.3 Photometric Model

Starting with the first images from the Apollo missions, a large number of Lunar reflectance models were studied [9, 10, 11]. In this work the reflectance is derived from the Lunar-Lambertian model [9, 12]. As shown in Figure 8, we define the following unit vectors: $\mathbf{n}$ is the local surface normal; $\mathbf{l}$ and $\mathbf{v}$ are directed at the locations of the Sun and the spacecraft, respectively, at the time when the image was captured. We

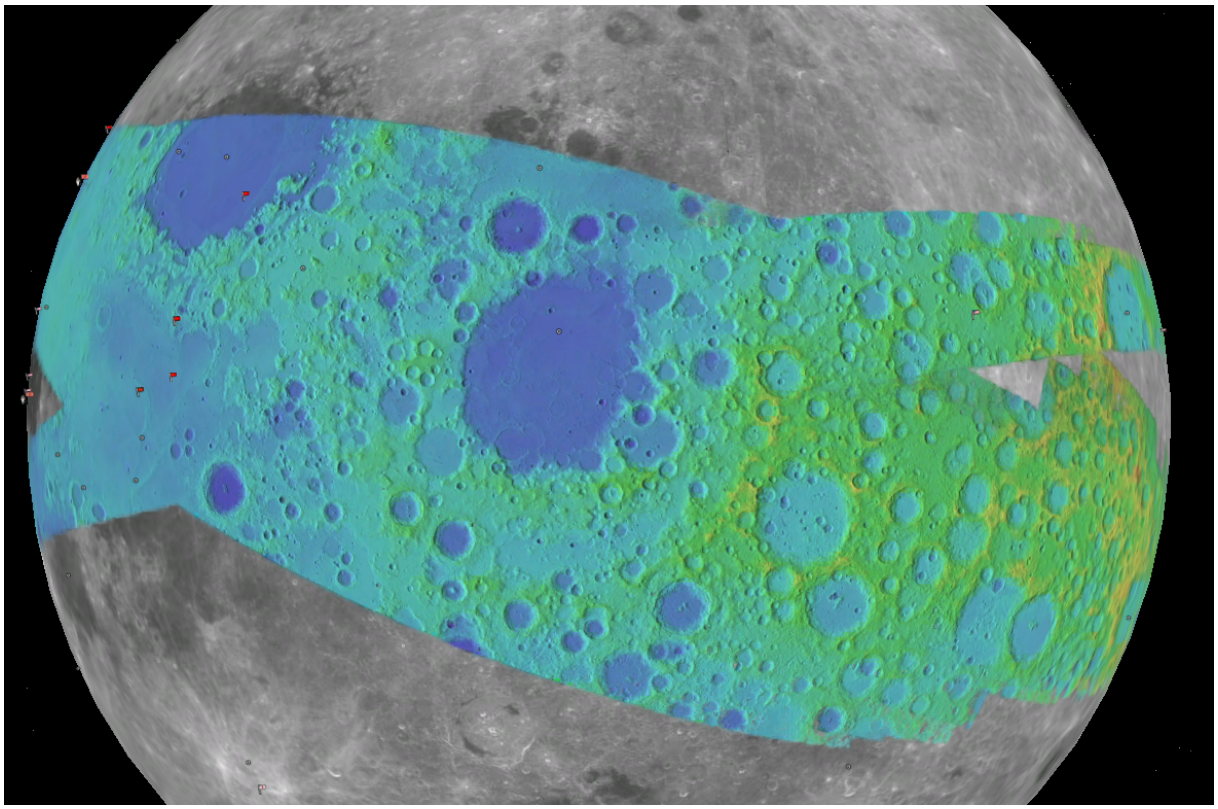

Figure 5: Colorshade of the enhanced digital terrain model of the Apollo zone.

further define the angles $\mathbf{i}$ separating $\mathbf{n}$ from $\mathbf{l}$, $\mathbf{e}$ separating $\mathbf{n}$ from $\mathbf{v}$, and the phase angle α separating $\mathbf{l}$ from $\mathbf{v}$.

The reflectance model used in our approach is given by

$$R_{ij}^k = (e^{-c_1\alpha} + c_2)\left[(1 - L(\alpha))\cos(\mathbf{i}_{ij}^k) + 2L(\alpha)\frac{\cos(\mathbf{i}_{ij}^k)}{\cos(\mathbf{i}_{ij}^k) + \cos(\mathbf{e}_{ij}^k)}\right] \quad (1)$$

where $L(\alpha)$ is a weighting factor between the Lunar and Lambertian reflectance models [13] that depends on the phase angle and surface properties. R is a photometric function that depends on the angles α, i and e. The parameters c_1 and c_2 play a significant role in modeling the surface reflectance at low phase angles. This can be noticed in the reduction of the banding artifacts in Figure 4 top right.

3.4 Albedo Reconstruction

The computation of the "R map" using Equation 1 and shown in Figure 3 is central to the albedo reconstruction technique. Let I_{ij}, A_{ij}, R_{ij} be the pixel value, albedo and R function at image location (i, j), and T be a variable proportional to the exposure time of the image. Then

$$I_{ij} = TA_{ij}R_{ij}. \quad (2)$$

Note that the image formation model described in Equation 2 does not take into consideration the camera transfer function since the influence of the non-linearities of the camera transfer function plays a secondary role in the image formation model [13]. From Equation 2 it can be seen that when the observed pixel value, exposure time, and R value are known, the image formation model in Equation 2 provides a unique

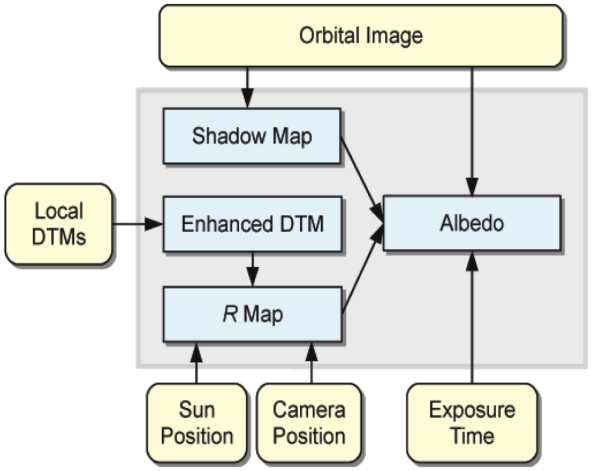

Figure 6: Overall system of the albedo reconstruction system.

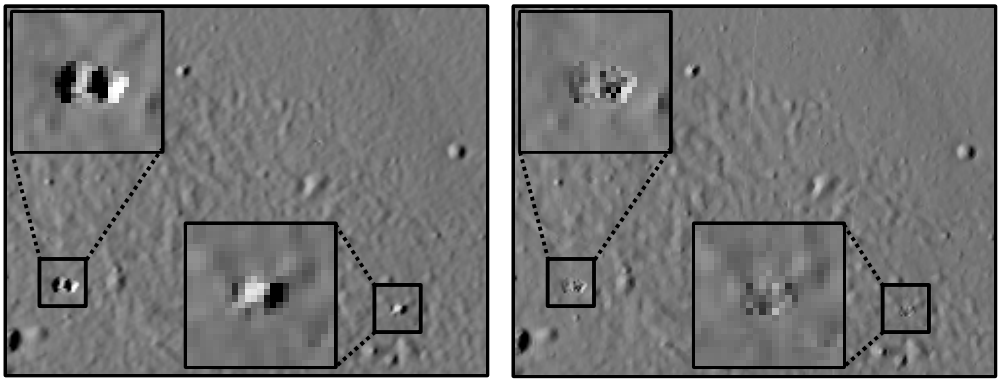

Figure 7: Hill-shaded maps generated using (left) single local DTM and (right) denoised DTM derived from multiple overlapping local DTM. Our denoising approach preserves the structure while reducing the artifacts shown in the insets.

albedo value. However, these values are subject to errors arising from measurement (exposure time), scanning (image value) or stereo modeling errors (reflectance), resulting in imprecise albedo calculations. The method presented here mitigates these errors by reconstructing the albedo of the Lunar surface from *all* the overlapping images, along with their corresponding exposure times and DTM information. The albedo reconstruction is formulated as the least squares problem that minimizes the following cost function $\mathbf{Q}$:

$$\mathbf{Q} = \sum_k \sum_{ij} \left[(I_{ij}^k - A_{ij} T^k R_{ij}^k)^2 S_{ij}^k w_{ij}^k \right] \tag{3}$$

where the superscript k denotes the variables associated with the kth image and S_{ij}^k is a shadow binary variable. $S_{ij}^k = 1$ when the pixel is in shadow and 0, otherwise. The weights w_{ij}^k are chosen such that they have linearly decreasing values from the center of the image ($w_{ij}^k = 1$) to the image boundaries ($w_{ij}^k = 0$). The choice of these weights insures that the reconstructed albedo mosaic is seamless. The optimal albedo reconstruction [14] from multiview images and their corresponding DTM is formulated as a minimization problem of finding

$$\{\tilde{A}_{ij}, \tilde{T}^k, \tilde{c}_l\} = \arg \min_{A_{ij}, T^k, c_l} \mathbf{Q} \tag{4}$$

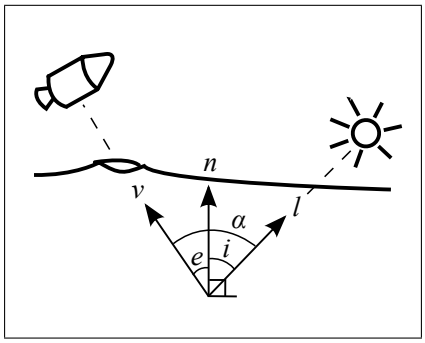

Figure 8: Illumination and viewing angles used by the Lunar-Lambertian reflectance model.

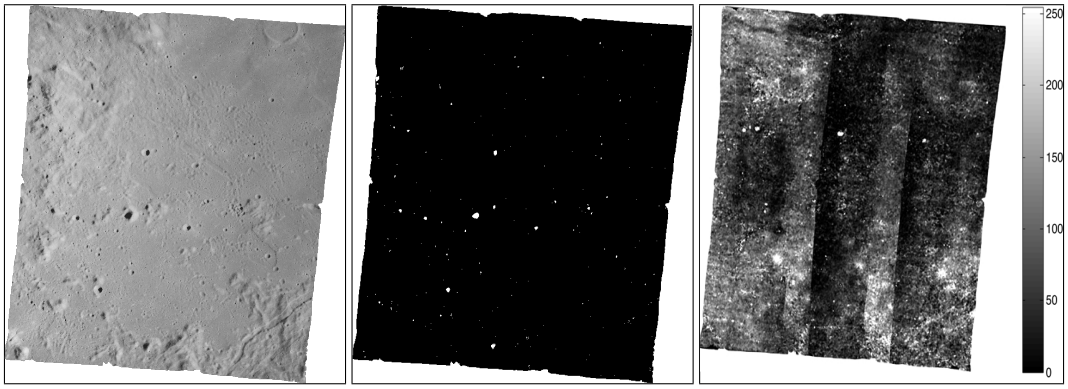

Figure 9: Orbital image: (left) input image, (middle) binary shadow map with shadow regions shown in white, (right) DEM confidence map (brighter areas have higher estimated error).

for all pixels ij and images k, where $\mathbf{Q}$ is the cost function in Equation 3. An iterative solution to the above least square problem is given by the Gauss-Newton updates described below.

- **Step 1 (initialization)**: Compute the enhanced DTM as described in Section 3.2 and the weighting coefficients. Normalize the weights so that the sum of weights at each pixel is 1. Initialize the exposure time as inversely proportional to the average image reflectance. Initialize the phase coefficients c_1 and c_2 to some reasonable values. Initialize the albedo as the arg min of the cost function $\mathbf{Q}$ for fixed exposure time and phase coefficients

$$A_{ij} = \frac{\sum_k I_{ij}^k T^k R_{ij}^k S_{ij}^k w_{ij}^k}{\sum_k (T^k R_{ij}^k)^2 S_{ij}^k w_{ij}^k} \tag{5}$$

- **Step 2**: Re-estimate the exposure time using

$$\tilde{T}^k = T^k + \frac{\sum_{ij} (I_{ij}^k - A_{ij} T^k R_{ij}^k) A_{ij} R_{ij}^k S_{ij}^k w_{ij}^k}{\sum_{ij} (A_{ij} R_{ij}^k)^2 S_{ij}^k w_{ij}^k} \tag{6}$$

- **Step 3**: Re-estimate the phase coefficients using

$$\tilde{c_1} = c_1 + \frac{\sum_{ijk} (I_{ij}^k - A_{ij} T^k R_{ij}^k) A_{ij} T^k \frac{\partial R_{ij}^k}{\partial c_1} S_{ij}^k w_{ij}^k}{\sum_{ijk} \left(A_{ij} T^k \frac{\partial R_{ij}^k}{\partial c_1} \right)^2 S_{ij}^k w_{ij}^k} \tag{7}$$

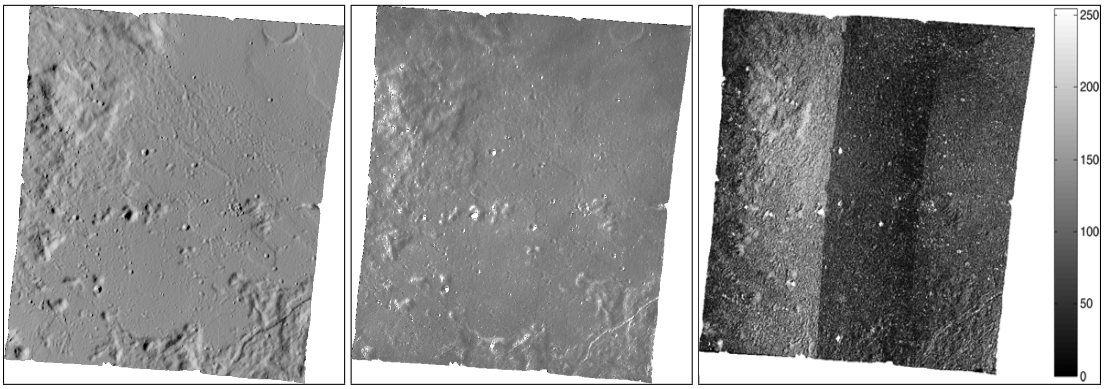

Figure 10: Albedo reconstruction: (left) R map, (middle) reconstructed albedo, (right) albedo confidence map (brighter areas have higher estimated error).

and analogously for c_2. The partial derivatives $\partial R_{ij}^k/\partial c_1$ and $\partial R_{ij}^k/\partial c_2$ are computed from Equation 1.

- **Step 4**: Re-estimate the albedo using

$$\tilde{A}_{ij} = A_{ij} + \frac{\sum_k (I_{ij}^k - A_{ij} T^k R_{ij}^k) T^k R_{ij}^k S_{ij}^k w_{ij}^k}{\sum_k (T^k R_{ij}^k)^2 S_{ij}^k w_{ij}^k} \tag{8}$$

- **Step 5**: Compute the error cost function **Q** for the re-estimated values of the albedo and exposure time.
- **Convergence**: If the convergence error between the consecutive iterations falls below a fixed threshold then stop. Otherwise return to step 2.
- **Step 6**: Estimate the precision of the albedo reconstruction at each pixel using the formula

$$E_{ij} = \frac{\sum_k (I_{ij}^k/(T^k R_{ij}^k) - A_{ij})^2 S_{ij}^k w_{ij}^k}{\sum_k w_{ij}^k} \tag{9}$$

4 Open Source Library: The Photometry Toolkit

The team of this proposal developed and released in open source a software library for albedo reconstruction that was used in the generation of these products, and which can be used in processing data from more recent Lunar missions including LRO-NAC data. The Photometry Toolkit is publicly available at https://github.com/NeoGeographyToolkit/PhotometryTK. Additional documentation on installation and usage is available at https://github.com/NeoGeographyToolkit/PhotometryTK/blob/master/docs/albedo.pdf

References

[1] Nefian, A., Husmann, K., Broxton, M., To, V., Lundy, M., Hancher, M.: A Bayesian formulation for sub-pixel refinement in stereo orbital imagery . International Conference on Image Processing (2009)

[2] Nefian, A.V., Smith, T., Moratto, Z., Kim, T., Beyer, R., Lundy, M., Fong, T.: Lunar albedo reconstruction from the metric camera images of the apollo 15 and 16 missions. NASA Lunar Science Institute Forum (2011)

[3] Nefian, A.V., Kim, T., Broxton, M., Beyer, R., Moratto, Z.: Towards albedo reconstruction from Apollo Metric Camera imagery. In: Lunar and Planetary Sci. Conf. (LPSC). (2010)

[4] Nefian, A., Kim, T., Moratto, Z., Beyer, R., Fong, T.: Lunar terrain and albedo reconstruction of the apollo 15 zone. International Symposium on Visual Computing (2010)

[5] Marvin Smith, Ara Nefian, G.B., Fong, T.: Outlier removal in stereo reconstructions of orbital images. International Symposium on Visual Computing (2010)

[6] Nefian, A., Alexandrov, O., Moratto, Z., Kim, T., Beyer, R., Fong, T.: Lunar Albedo Reconstruction From Apollo Metric Camera Imagery. Planetary Data: A Workshop for Users and Software Developers, Flagstaff, Arizona (2012)

[7] Arévalo, V., González, J., Ambrosio, G.: Shadow detection in colour high-resolution satellite images. Int. J. Remote Sens. **29** (2008) 1945–1963

[8] Matthies L., H., Cheng, Y.: Stereo vision and shadow analysis for landing hazard detection. IEEE International Conference on Robotics and Automation (2008) 2735 – 2742

[9] McEwen, A.S.: Photometric functions for photoclinometry and other applications. Icarus **92** (1991) 298–311

[10] McEwen, A.S.: A precise lunar photometric function. Lunar and Planet. Sci. Conf. 27th (1996)

[11] Minnaert, M.: The reciprocity principle in lunar photometry. Journal of Astrophysics (1941)

[12] McEwen, A.S.: Exogenic and endogenic albedo and color patterns on Europa. Journal of Geophysical Research **91** (1986) 8077–8097

[13] Gaskell, R.W., Barnouin-Jha, O.S., Scheeres, D.J., Konopliv, A.S., Mukai, T., Abe, S., Saito, J., Ishiguro, M., Kubota, T., Hashimoto, T., Kawaguchi, J., Yoshikawa, M., Shirakawa, K., Kominato, T., Hirata, N., Demura, H.: Characterizing and navigating small bodies with imaging data. Meteoritics and Planetary Science **43** (2008) 1049–1061

[14] Yuille, A., Snow, D.: Shape and albedo from multiple images using integrability. In: CVPR '97: Proceedings of the 1997 Conference on Computer Vision and Pattern Recognition (CVPR '97), Washington, DC, USA, IEEE Computer Society (1997) 158